

Quantum Manifestations of Graphene Edge Stress and Edge Instability: A First-Principles Study

Bing Huang¹, Miao Liu², Ninghai Su², Jian Wu¹,
Wenhui Duan¹, Bing-lin Gu¹, and Feng Liu^{2*}

¹*Department of Physics, Tsinghua University, Beijing 100084, China and*

²*Department of Materials Science and Engineering,
University of Utah, Salt Lake City, Utah 84112*

(Dated: November 5, 2018)

Abstract

We have performed first-principles calculations of graphene edge stresses, which display two interesting quantum manifestations absent from the classical interpretation: the armchair edge stress oscillates with nanoribbon width and the zigzag edge stress is noticeably reduced by spin polarization. Such quantum stress effects in turn manifest in mechanical edge twisting and warping instability, showing features not to be captured by empirical potentials or continuum theory. Edge adsorption of H and Stone-Wales reconstruction are shown to provide alternative mechanisms in relieving the edge compression and hence to stabilize the planar edge structure.

PACS numbers: 71.15.Mb,62.25.-g,61.46.-w,81.05.Tp

* Email: fliu@eng.utah.edu

Graphene, a two-dimensional (2D) single layer of carbon atoms, has attracted tremendous attention because of its unique electronic properties[1] and potential applications in electronic devices[2]. Earlier studies have focused on characterizing the unusual electronic and transport properties of graphene, particularly as a massless Dirac fermion system[1, 2]. More recently, some attention has been shifted to the structural stability of graphene[2–5], which is critically important to realizing the potential applications of graphene. On the one hand, as a 2D membrane structure, graphene provides an ideal testing ground[3, 4] for the classical Mermin-Wagner theorem on the existence of long-range crystalline order in 2D[6, 7]. On the other hand, the free edges of graphene are amenable to edge instabilities[5, 8–10].

The graphene edge stability is characterized by two fundamental thermodynamic quantities: edge energy and edge stress. The edge of a 2D structure can be understood in analogy to the surface of a 3D structure[11, 12]: the edge (surface) *energy* accounting for the energy cost to create an edge (surface) defines the edge (surface) *chemical* stability; the edge (surface) *stress* accounting for the energy cost to deform an edge (surface) defines the edge (surface) *mechanical* stability. First-principles calculations showed that chemically the armchair edge is more stable with a lower energy, while the zigzag edge is metastable against reconstruction[8], and both edges are hydrogenated in an H-rich environment[9]. Empirical-potential calculations showed that both intrinsic edges are under compressive stress rendering a mechanical edge twisting and warping instability[10].

Usually, stress and mechanical instability are understood as phenomena of classical mechanics, but they are expected to be affected by quantum effects which become prominent at nanoscale. So far, however, quantum effects have been mostly shown for electronic structure and energetic quantities of low-dimensional nanostructures. Here, we demonstrate an interesting example of quantum manifestations of mechanical quantities in graphene edge stress. Using first-principles calculations, we predict that the armchair edge stress in a nanoribbon exhibits a large oscillation with ribbon width arising from quantum size effect, while the zigzag edge stress is reduced by spin polarization. Such quantum effects on edge stress in turn manifest in graphene edge mechanical instability, with "quantum" features that apparently cannot be described by empirical force-field potentials or continuum theory.

Our calculations were performed using the method based on density functional theory (DFT) in the generalized gradient approximation, with the Perdew-Burke-Ernzerhof functional for electron exchange and correlation potentials, as implemented in the VASP code

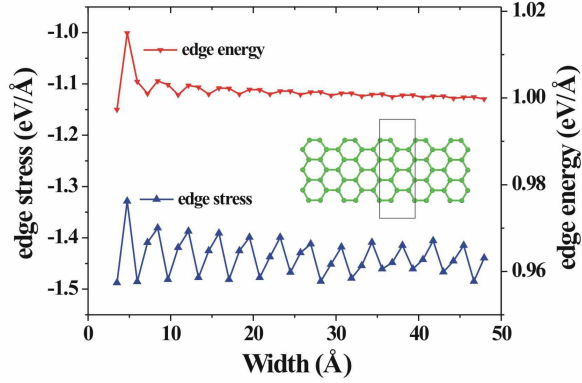


FIG. 1: The armchair edge stresses and edge energies of graphene nanoribbons as a function of ribbon width. Inset: schematics of the nanoribbon; the rectangle marks one unit cell (supercell) of the ribbon.

[13]. The electron-ion interaction was described by the projector augmented wave method, and the energy cutoff was set to 500 eV. The structures were fully optimized using the conjugate gradient algorithm until the residual atomic forces to be smaller than 10 meV /Å. The supercell method with periodic boundary conditions was adopted to model the graphene nanoribbons (GNR), with a vacuum layer larger than 15 Å to guarantee that there was no interaction between the GNR images in the neighboring cells. The edge energy is calculated as $E_{edge} = (E_{ribbon} - E_{atom})/2L$, where E_{ribbon} is the total energy of the graphene nanoribbon in the supercell, E_{atom} is the energy per atom in a perfect graphene without edge, and L is the length of edge. The edge stress is calculated as $\sigma_{edge} = \sigma_{xx}/2L$, where σ_{xx} is the diagonal component of supercell stress tensor in the x -direction (defined along the edge), which is calculated using the Nielsen-Martin algorithm [14]. All other components of stress tensor vanish. We also note that DFT is suitable for calculating ground-state properties of lattice energies and stresses, to which the non-local many-body effects are not expected to be important.

Figure 1 shows the calculated edge energy and edge stress of GNR armchair edges as a function of ribbon width ranging from ~ 3.5 to ~ 48 Å. One notices that both edge energy and edge stress oscillate with the increasing width having a period of 3 but out of phase with each other. The oscillations are originated from the quantum confinement effect, as also manifested in the similar oscillations of electron band structures[15–18]. The

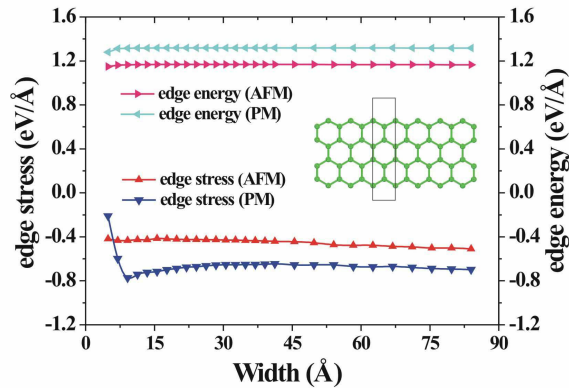


FIG. 2: The AFM and PM zigzag edge stresses and edge energies of graphene nanoribbons as a function of ribbon width. Inset: schematics of the nanoribbon; the rectangle marks one unit cell (supercell) of the ribbon.

oscillation magnitude of edge energy decays quickly with the increasing width and converges to ~ 1.0 eV/Å, which agrees well with the previous first-principles values[8]. In contrast, the oscillation magnitude of edge stress decays much slower with a mean value of ~ -1.45 eV/Å (using negative sign as convention for compressive stress). The much larger oscillation in edge stress than in edge energy is possibly caused by the fact that edge stress equals to the derivative of edge energy with respect to strain, so that stress is much more sensitive to the width-dependent quantum confinement effect. There is also a slight revival effect in the stress oscillations at ~ 40 Å width, whose origin is not clear and needs further study.

Figure 2 shows the calculated edge energy and edge stress of GNR zigzag edges as a function of ribbon width ranging from ~ 5.0 to ~ 85 Å. In this case, both edge energy and edge stress show very weak width dependence and converges quickly, again consistent with their corresponding electronic-structure behavior[15–18]. However, the zigzag edge is known to have an antiferromagnetic (AFM) ground state[17]. The AFM edge energy is calculated to be ~ 1.2 eV/Å, about 0.2 eV/Å lower than the paramagnetic (PM) edge energy[8, 9, 19]. Thus, we have calculated the edge stress of both AFM and PM states for comparison. We found that spin polarization have a sizable effect reducing the compressive stress from ~ -0.7 eV/Å in the PM edge to ~ -0.5 eV/Å in the AFM edge.

Our first-principles stress calculations confirm qualitatively the recent empirical-potential results[10] that both edges are under compressive stress. However, there are also some

significant differences. Two quantum manifestations of edge stress stand out, which are absent from the empirical prediction. One is the quantum oscillation of armchair edge stress with the increasing nanoribbon width, and the other is the reduction of zigzag edge stress by spin polarization. The physical origin of edge energy and edge stress is associated with the formation of one dangling bond on each edge atom. The repulsive interaction between the dangling bonds is believed to be one origin for the 'compressive' edge stress. In addition, in the armchair edge, it is well-known[20] that the edge dimers form triple $\text{-C}\equiv\text{C-}$ bonds with a much shorter distance ($\sim 1.23 \text{ \AA}$ according to our calculation) adding extra compressive stress to the edge; while in the zigzag edge, spin polarization further reduces the compressive stress. Therefore, quantitatively, the armchair edge has a much larger compressive stress ($\sim -1.45 \text{ eV/\AA}$) than the zigzag edge ($\sim -0.5 \text{ eV/\AA}$). In contrast, the empirical potentials predicted a smaller compressive stress in the armchair edge ($\sim -1.05 \text{ eV/\AA}$) than in the zigzag edge ($\sim -2.05 \text{ eV/\AA}$)[10].

The quantum effects in edge stress will in turn modify the mechanical edge instability. The compressive edge stress means the edge has a tendency to stretch. If we apply a uniaxial in-plane strain to a nanoribbon along the edge direction, the strain energy can be calculated as [10]

$$E_{str} = 2\tau_e L \varepsilon + E_e L \varepsilon^2 + \frac{1}{2} E_s A \varepsilon^2 \quad (1)$$

Here, A is the ribbon area, L is the edge length, τ_e is the edge stress, E_e is the 1D edge elastic modulus in a 2D nanoribbon, in analogy to the 2D surface elastic modulus in a 3D nanofilm[21], and E_s is the 2D sheet elastic modulus. Since τ_e is negative, for small enough tensional strain ε (positive), the negative first term (linear to ε) in Eq. (1) can always overcome the positive second and third terms (quadratic to ε) to make E_{str} negative. Consequently, the ribbon is unstable against a small amount of stretching along the edge direction. Fitting first-principles calculations, by manually deforming the sheet and ribbon along the edge direction, to equation (1), we obtained $E_s \approx 21.09 \text{ eV/\AA}^2$, $E_e(\text{amchair}) \approx 3 \text{ eV/\AA}$ and $E_e(\text{zigzag}) \approx 24 \text{ eV/\AA}$ with τ_e already calculated above directly (see Figs. 1 and 2). Our E_s value is in good agreement with the experiment[22] and empirical simulation result[10]. But our E_e values are notably different from the empirical results[10].

Another effective way to stretch the edge of a 2D sheet is by out-of-plane edge twisting and warping motions, which are barrierless processes. For example, assuming a sinusoidal

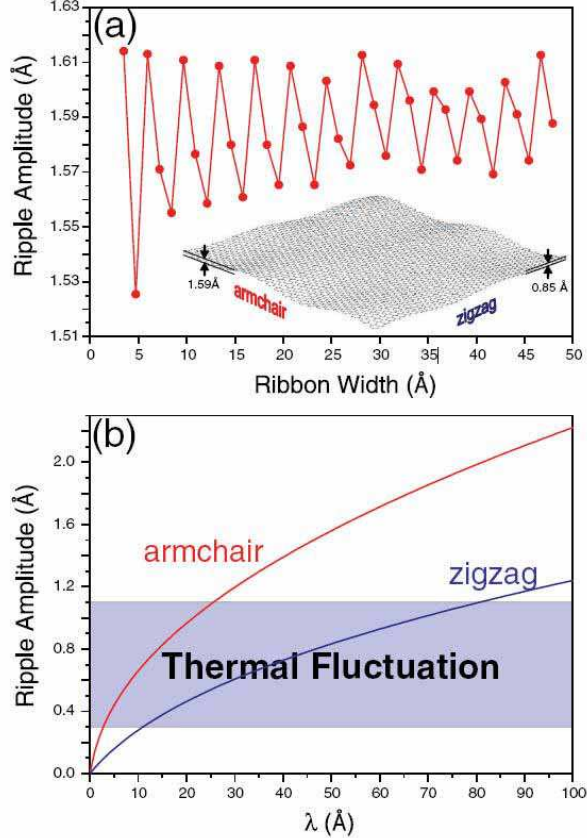


FIG. 3: (a) Armchair edge ripple amplitude versus ribbon width for $\lambda = 50\text{\AA}$. Inset: Schematics of ripple formation along the armchair and zigzag edge for $\lambda = 50\text{\AA}$. (b) Armchair (red) and zigzag (blue) edge ripple amplitude as a function of λ . Light blue band shows the typical range of thermal fluctuation.

edge warping with displacement $\mu_e = a \sin(2\pi x/\lambda)$ of amplitude a and wavelength λ , which decays exponentially into the sheet as $e^{-y/l}$ (See inset of Fig. 3), where l is the decay length, Shenoy *et al.* have shown that minimization of strain energy leads to characteristic length scales of such warping instability as $l \approx 0.23\lambda$ and $a \approx \sqrt{(-\lambda\tau_e)/(1.37E_b + 14.8E_e/\lambda)}$. Using their empirical-potential values of τ_e , E_e and E_s , they estimated that the warping magnitude of armchair edge is smaller than that of zigzag edge and both are larger than typical thermal fluctuations[10].

Our first-principle predictions, however, are different in several ways. First, absent from empirical prediction, the quantum oscillation of τ_e of armchair edge gives rise to an oscillating armchair edge warping amplitude for given wavelength as a function of nanoribbon width, as shown in Fig. 3a. Second, opposite to empirical prediction, the warping amplitude of

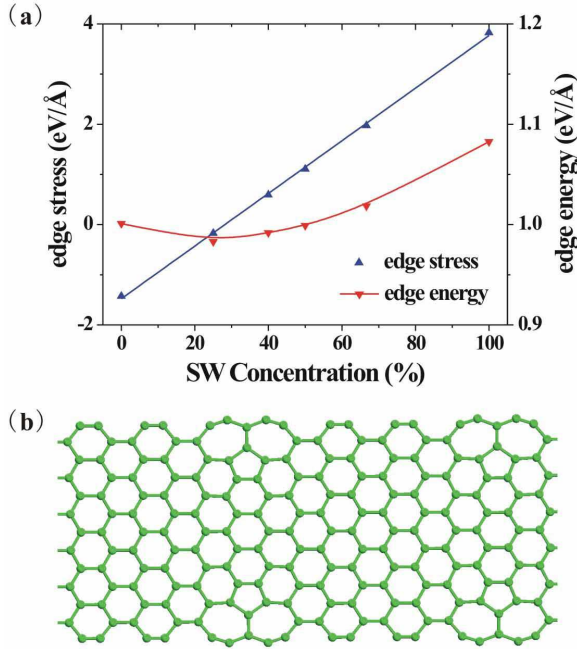


FIG. 4: (a) The armchair edge stresses (with linear fit) and edge energies of graphene nanoribbons as a function of edge SW defect concentration. (b) The optimized ribbon structure at the 50% SW defect concentration.

armchair edge is much larger than that of zigzag edge, as shown in Figs. 3b. Third, the mechanical undulation of zigzag edges induced by compressive edge stress is comparable to thermal fluctuations[3, 4], as shown in Fig. 3b, and hence the two are difficult to distinguish. We also note that in addition to the continuum analysis we perform here, the accurate first-principles values of τ_e and E_e can be used as input parameters for the finite element simulations of large graphene systems[10].

Because the compressive edge stress is partly originated from the dangling bond, naturally, we may saturate the dangling bonds to relieve the compressive stress. We have tested this idea by saturating the edge with H that indeed confirmed our physical intuition. For armchair edge in a 1-nm wide ribbon, we found H saturation changes the edge stress from -1.42 eV/\AA to -0.35 eV/\AA ; for zigzag edge in a 2.0-nm wide ribbon, it changes the edge stress from -0.42 eV/\AA to $+0.13 \text{ eV/\AA}$. Therefore, the H edge saturation, or saturation by other molecules in general, is expected to relieve the edge compression. Especially, it can reverse the compressive stress in a zigzag edge to tensile.

Surface reconstruction has long been known as an effective mechanism in relieving surface

stress[23]. Thus, in addition to H saturation, we have investigated possible edge reconstructions in relieving the edge compressive stress. We have considered the Stone-Wales (SW) defect[24], which appeared to us become a SW defect in 2D is equivalent to a dislocation core in 3D that is known as a common stress relieve mechanism. Figure 4a shows the calculated armchair edge stress along with edge energy as a function of one type of SW defect (7-5-7 ring structure) concentration. Figure 4b shows an example of the optimized edge structure at the 50% defect concentration. One sees from Fig. 4a that the edge stress increases linearly from compressive to tensile with the increasing SW defect concentration. The most stable edge structure is at $\sim 25\%$ defect concentration where the edge stress is very small and slightly compressive. A small stress value indicates that this chemically stable edge structure (with the lowest edge energy) is also most mechanically stable against deformation.

Figure 5a shows the ground-state AF zigzag edge stress along with edge energy as a function of another type of SW defect (5-7 ring structure) concentration. Figure 5b shows an example of the optimized edge structure and spin charge density at the 50% defect concentration. Again, the edge stress increases linearly from compressive to tensile with the increasing defect concentration, the same as the case of armchair edge (Fig. 4a), but the edge energy decreases monotonically with the most stable edge having 100% of defects, in agreement with a recent first-principles calculation [8]. The initial compressive edge stress (~ -0.5 eV/Å) is completely reversed to a large tensile value of ~ 1.2 eV/Å in the most stable edge. Also, the 100% defected edge becomes non-spin-polarized. In general, the zigzag edge spin decreases continuously with the increasing SW defect concentration, similar to the behavior found previously for other types of defects [25].

We note that there is a first-principles calculation of graphene edge stress was reported recently[26], but that calculation appears inconsistent with all other existing first-principles calculations . Their edge energies differ from all previous results[8, 9] and ours that are consistent with each other. The well-known spin-polarization of the zigzag edge was not considered, the quantum oscillation of armchair edge energy and stress was not shown, and their edge stress were not calculated from direct quantum-mechanical formula [14].

In conclusion, quantum effects have been widely shown for electronic structure and energetic quantities of low-dimensional nanostructures. We demonstrate, in addition, quantum manifestations of mechanical quantities in graphene edge stress. We show that quantum confinement can lead to stress oscillations and spin polarization can reduce stress, which in

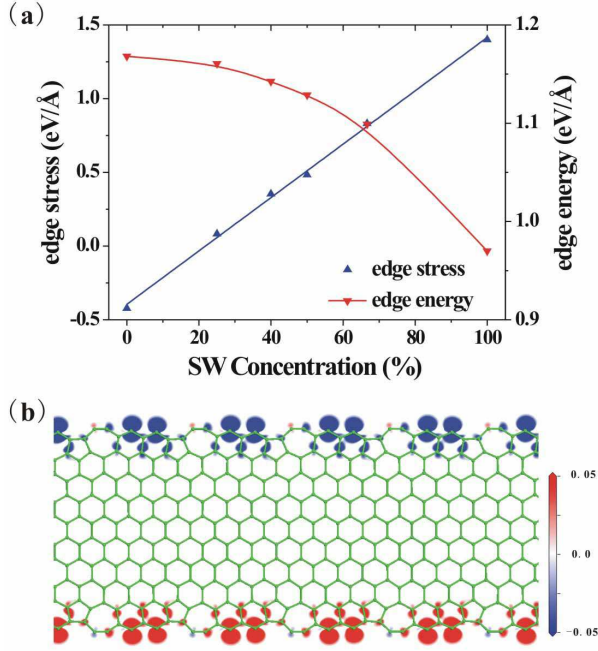


FIG. 5: (a) The zigzag edge stresses (with linear fit) and edge energies of graphene nanoribbons as a function of SW defect concentration. (b) The optimized ribbon structure and spatial distribution of spin density (charge density difference between spin-up and spin-down states in units of $\mu_B \text{ \AA}^{-2}$) of the AFM ground state at the 50% SW defect concentration.

turn "quantum mechanically" modify the edge twisting and warping instability. We further show that H edge saturation and SW edge reconstruction can not only improve the 'chemical' stability of graphene edges by lowering the edge energy as shown before[8, 9], but also enhance their 'mechanical' stability by converting compressive edge stress towards tensile and hence stabilizing the planar edge structure. Our first-principles findings, which cannot be captured by classical methods, provide new insights to the understanding of mechanical stability of graphene. We suggest that experimental measurement of armchair edge ripple magnitudes for different widths and comparison with zigzag edge ripples could confirm our predictions of quantum effects in graphene edge stresses differentiating from empirical results. We expect the quantum manifestation of mechanical properties such as stress to exist generally in many low-dimensional nanostructures.

The work at Tsinghua is supported by the Ministry of Science and Technology of China

and NSFC, the work at Utah is supported by DOE.

- [1] A. H. Castro Neto *et al.*, Rev. Mod. Phys. **81**, 109 (2008).
- [2] A. K. Geim and K. S. Novoselov, Nature Mater. **6**, 183 (2007).
- [3] J. C. Meyer *et al.*, Nature (London) **446**, 60 (2007).
- [4] A. Fasolino, J. H. Los and M. I. Katsnelson, Nature Mater. **6**, 858 (2007).
- [5] M. S. Gass *et al.*, Nature Nanotech. **3**, 676 (2008).
- [6] L. D. Landau, Phys. Z. Sowjetunion **11**, 26 (1937).
- [7] N. D. Mermin, Phys. Rev. **176**, 250 (1968).
- [8] P. Koskinen, S. Malola, and H. Hakkinen, Phys. Rev. Lett. **101**, 115502 (2008).
- [9] T. Wassmann *et al.*, Phys. Rev. Lett. **101**, 096402 (2008).
- [10] V. B. Shenoy, C. D. Reddy, A. Ramasubramaniam, and Y.W. Zhang, Phys. Rev. Lett. **101**, 245501 (2008).
- [11] F. Liu, M. Hohage, and M. G. Lagally, Encyclopedia of Appl. Phys., eds. H. Immergut and G. Trigg, Supplement Volume, **321** (1999).
- [12] R. Pala and F. Liu, J. Chem. Phys. **120**, 7720 (2004).
- [13] G. Kresse and J. Furthmüller, Comput. Mater. Sci. **6**, 15 (1996).
- [14] O. H. Nielsen and R. M. Martin, Phys. Rev. B **32**, 3780 (1985).
- [15] K. Nakada *et al.*, Phys. Rev. B **54**, 17954 (1996).
- [16] K. Wakabayashi *et al.*, Phys. Rev. B **59**, 8271 (1999).
- [17] Y.-W. Son, M. L. Cohen, and S. G. Louie, Phys. Rev. Lett. **97**, 216803 (2006).
- [18] Q. Yan *et al.*, Nano Lett. **7**, 1469 (2007).
- [19] H. Lee *et al.*, Phys. Rev. B, **72**, 174431 (2005).
- [20] T. Kawai, Y. Miyamoto, O. Sugino, and Y. Koga, Phys. Rev. B, **62**, 16349 (2000).
- [21] J. Zang and F. Liu, Nanotechno. **18**, 405501 (2007); Appl. Phys. Lett. **92**, 021905 (2008).
- [22] C. Lee *et al.*, Science **321**, 385 (2008).
- [23] F. Liu and M.G. Lagally, Phys. Rev. Lett. **76**, 3156 (1996).
- [24] A. J. Stone and D. J. Wales, Chem. Phys. Lett. **128**, 501 (1986).
- [25] B. Huang *et al.*, Phys. Rev. B, **77**, 153411 (2008).
- [26] S. Jun, Phys. Rev. B, **78**, 073405 (2008).